Int. J. Electrochem. Sci., 7 **(2012)** 10884 - 10893

International Journal of
ELECTROCHEMICAL
SCIENCE
www.electrochemsci.org

Synthesis of a Novel Catalyst via Pyrolyzing Melamine with Fe Precursor and Its Excellent Electrocatalysis for Oxygen Reduction

Tao Yang[*], *Guiquan Han*

School of Chemical Engineering,Huaihai Institute of Technology,Lianyungang 222005, China.
[*]E-mail: yangtao_hit@163.com

Received: 17 June 2012 / *Accepted:* 24 September 2012 / *Published:* 1 November 2012

In this paper, a non-noble metal catalyst based on ferric chloride and melamine is synthesized via pyrolyzing in an inert atmosphere at 900 ℃. The existence of Fe is demonstrated by X-ray diffraction analysis. The microstructure of the nitrogen containing carbon is investigated by the transmission electron microscopy. The bonding configurations of the surface nitrogen atoms are determined by X-ray photoelectron spectroscopy technique. The steady-state electrocatalysis for oxygen reduction is studied by the rotating disk electrode tests. We find that the nitrogen atoms in the carbon network are dominantly in the form of pyridinic nitrogen. The catalyst displays excellent performance evidenced by a high onset potential of 0.88 V for oxygen reduction reaction. As for the practical application in H_2-O_2 fuel cell, a power density as high as 418.20 mW cm^{-2} is achieved at 1100 mA cm^{-2} (at 25 ℃) without humidification. These results imply the potential application of melamine as a nitrogen precursor in Fe based catalysts for oxygen reduction reaction.

Keywords: Fe catalyst; oxygen reduction reaction; proton exchange membrane fuel cell; melamine

1. INTRODUCTION

Proton exchange membrane fuel cells (PEMFCs) have received much attention because of their advantages such as high energy density and low pollution [1, 2]. Much research has been concentrated on the studies of the key components of PEMFCs. The development of electrocatalyst is one of the most researchful hotspots on the basis of their significant electrocatalysis [3, 4]. Traditionally, the electrocatalyst at both the anode and cathode of PEMFC is commonly achieved from the precious metals of platinum or platinum alloys. According to the nearest cost analysis, the catalysts are by far the most costly component, amounting to more than 50 percent of the PEMFC stack cost. As Pt gets even scarcer and more expensive, the share of catalysts cost will soar in the near future [5, 6]. Thus,

much work has been devoted to the non-precious metal catalysts that own the advantages of high oxygen reduction reaction (ORR) activity and low cost simultaneously. Since the first research of cobalt phthalocyanine as a non-noble catalyst for the ORR in 1965, exploring transition metal catalyst has become one of the most feasible ways to seeking suitable replacements for Pt and Pt-base catalysts [7-9]. During the past decades, many efforts have been focused on the various transition type metals [10, 11]. Fe has been considered to be one of the most promising candidates for the following causes [12]. Firstly, Fe can be introduced into the carbon framework easily via pyrolyzing ferric salt in an inert atmosphere. Secondly, the presence of Fe catalyzes the process of carbon graphitization at a slightly lower temperature. Thirdly, Fe exhibits higher electrocatalysis than the other transition metal investigated [10].

As far as we known, the formation of FeN_4 moiety heavily contributes to the ORR activity of Fe catalysts [13]. The incorporation of nitrogen atoms can also be obtained by pyrolyzing carbon samples with nitrogen precursors in an inert atmosphere. Nitrogen atoms are then bonded onto the graphite network in the forms of pyridinic, pyrrolic and quaternary nitrogen. The lone electron pairs of nitrogen atoms contribute to form a delocalized conjugated system with the adjacent sp^2-hybridized carbon network [14] resulting in great improvement in ORR activity.

Fe catalysts are by far the most promising non-precious metal catalysts for ORR which has been assumed to consist of an iron cation coordinated by four pyridinic nitrogen atoms attached to the edges of graphitic crystallites [15]. However, the previous reports demonstrates that it is impossible to only produce pyridinic nitrogen because of the autonomous transformation between the pyridinic and quaternary nitrogen, and the equilibrium will shift to the latter at higher temperature. Therefore, N precursors rich in pyridinic nitrogen might be more desirable than other nitrogen compounds.

Melamine, a simple and cheap chemical with a high N content of 67 wt%, has been used as a nitrogen precursor to modulate graphene framework [16]. Nallathambi revealed that the performance of Fe catalyst prepared from melamine far exceed those from bipyridine, pyrazine and purine at the same N loading. Nallathambi demonstrated that the N/C ratio of nitrogen precursor was the key effect contributing to the electrocatalysis, which was assumed to increase the accessible active site density by reducing carbon deposition in the pores of the carbon support during the pyrolysis procedure [17]. However, the microstructure of the catalyst and the configuration of nitrogen groups are not revealed. Sheng synthesized nitrogen doped graphene by thermal decomposing graphite oxide with melamine. A high nitrogen content of 10.1 % (atom %) was successfully obtained when the mass ratio of graphite oxide and melamine was 1:5 and the heat treatment was carried out at 700 ℃ [18].

In this paper, we report a Fe catalyst synthesized by thermal pyrolyzing carbon-supported ferrous precursor and melamine. Electrochemical performance and structural characteristics of the prepared catalysts are measured.

2. EXPERIMENTAL

2.1 Catalyst synthesis

In a typical procedure, the acid-treated carbon support (Ketjen carbon black EC 300J, 0.40 g) and $FeCl_3 \cdot 6H_2O$ (0.20 g) were ultrasonically dispersed in de-ionized water. The suspension was

vacuum-dried and ground with melamine (1.00g). The mixture was then undergone a heat-treatment at 900 °C in nitrogen atmosphere for 1 hour. The nominal mass ratio of C: Fe: N is 17.5: 1: 17.5 according to the thermal decomposition in high temperature. The heat-treated sample was subsequently pre-leached in 0.5 M H_2SO_4 at 80°C for 8 hours and thoroughly washed in de-ionized water. Finally, the catalyst was heat-treated again in nitrogen atmosphere for 3 hours. A Fe free N-C sample and a nitrogen free Fe-C catalyst free of nitrogen were produced in the same way to comparison,

2.2 Physical characterization

The crystallinity of the as prepared samples was determined by X-ray diffraction (XRD) with a Cu Ka radiation source and a graphite monochromator. The bonding configurations of surface nitrogen groups were characterized by X-ray photoelectron spectroscopy (XPS). The microstructure was demonstrated by transmission electron microscope technique on a JEOL JEM-2100 microscope operating at 200 kV.

2.3 Electrochemical measurements and fuel cell tests

A glassy carbon electrode (GCE, 0.25 cm^2) covered with thin catalyst layer was used as work electrode. 10 mg catalyst and 100 μL of Nafion (5 wt.%) was ultrasonically dispersed in a solution of 600 μL ethanol and 300 μL water. 10 μL of the as prepared catalyst suspension then was dropped onto the GCE with micropipette. The GCE was dried in N_2 flow at room temperature. The rotating disk electrode (RDE) tests were performed in a conventional three electrode system at room temperature. Pt wire and saturated calomel electrode served as counter electrode and reference electrode respectively. All performance data reported in this paper were transformed to refer to the normal hydrogen electrode (NHE).

As to the practical performance test in fuel cell, a catalyst ink was prepared by ultrasonically dispersing catalyst powder and Nafion solution in the mixture of de-ionized water and isopropanol. Nafion content in the dry catalyst was kept at 30 wt.%. The catalyst ink was then applied to the cathode gas diffusion layer until the catalyst loading was 4 mg cm^{-2}. A commercially Pt-catalyst (Shanghai HeSen Ltd., Pt 40 wt.%) was used at anode (0.25 mg cm^{-2}) without any further treatment. The cathode and anode were hot pressed onto two sides of a Nafion 112 membrane. A MEA with a area of 4 cm^2 and a single-serpentine flow channel was used. Pure hydrogen and oxygen were supplied to the anode and cathode without humidification at a flow rate of 200 and 400 mL min^{-1}, respectively.

3. RESULTS AND DISCUSSION

3.1 XRD patterns

The XRD patterns of the Fe–N–C catalyst, the N-free Fe-C and the Fe-free C-N samples are shown in Fig.1. The broad peak at around 2 θ = 22.5-25.5℃ is assigned to the (002) characteristic

diffraction of the graphitic crystalline that are attributed to two existences of amorphous carbon and graphitic carbon [19, 20]. We can observe some variation when Fe and/or N are introduced. Compared to the Fe-free C-N sample, the Fe-C and Fe-C-N catalysts display much sharper and narrower carbon (002) peaks. This shape change implies a better graphitic crystalline structure probably enhanced by the presence of the transition metals [20]. Relative to Fe-C catalyst, the (002) peak of the Fe-C-N catalyst exhibits a slightly positive shift that indicates a reduced *d*-spacing of graphite planes. It has been reported that a significant nitrogen doping can lead to a more compact graphitic structure [21, 22]. The sharp peaks at around 2 θ = 42.5-44.5℃ of Fe containing catalysts correspond to the typical Fe (110) diffraction [20].

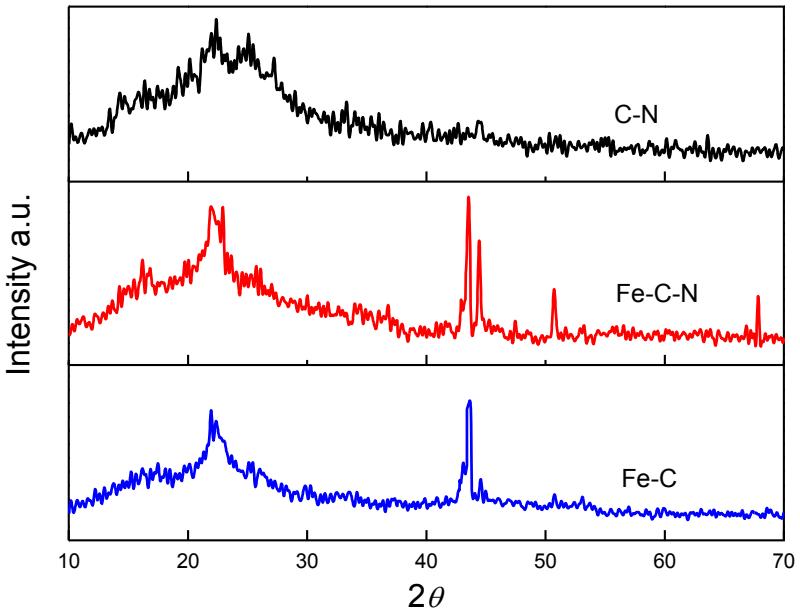

Figure 1. XRD patterns for non-precious metal catalyst samples after heat treatment and acid leach.

3.2 XPS analysis

The existence of surface nitrogen groups are demonstrated with XPS and displayed in Fig.2. The two pronounced nitrogen peaks at (400.8 eV) and (398.7 eV) can be attributed to the configurations of pyridinic and quaternary nitrogen, respectively, suggesting that the N atoms are successfully incorporated into the graphite framework. The pyridinic nitrogen (398.6 ± 0.3 eV) corresponds to the nitrogen atoms bonding onto the edges of the graphitic crystallites layers, and pyrrolic nitrogen (400.5 ± 0.3 eV) is defined as the nitrogen atoms in a five-membered ring structure. These two types of nitrogen atoms contribute to the conjugated system with a pair of *p*-electrons in the graphene layers. The quaternary nitrogen (401.3 ± 0.3 eV) is assigned to the nitrogen atoms replacing the carbon atoms in the graphitic crystallites plane [23]. According to the bond configuration and the location in the graphite crystallites, it has been concluded that the pyridine like nitrogen atoms are more suitable to coordinate with the transitional metals and form the active catalysts sites [18, 24]. However, it is impractical to produce pyridinic nitrogen only, because of the autonomous

transformation between the pyridinic and quaternary nitrogen during the thermal treatment [25, 26]. In addition, this equilibrium shifts to the quaternary nitrogen at a higher annealing temperature. Sheng found the ratio of pyridinic-N and quaternary-N decreased from 3.21 (40.19%: 12.52) to 1.82 (52.13: 28.59) as the pyrolysis temperature rising from 700 ℃ to 800 ℃[18]. In our research, the mass ratio of pyridinic nitrogen and quaternary nitrogen is 3.43 and 2.16 for C-N and Fe-C-N samples, respectively (Table 1). Our results also implies that the presence of Fe is able to push the equilibrium towards the quaternary nitrogen, which is consistent with Dr. Wu's report [27]. In our work, the total surface N content was 5.7 % and 5.3 % (atom ratio) for C-N and Fe-C-N samples, respectively. In Sheng's research, the total surface N loading was as high as 10.1 (atom ratio) when the mass ratio of graphite oxide and melamine was 1: 5 and synthesized at 700 ℃[18], while Nallathambi obtained the bulk N loading of 4.1 wt% when the nominal 6.3 wt% N (melamine) was used as nitrogen precursor and pyrolyzed at 800 ℃[17]. These difference in nitrogen content might be attributed to the different synthesis procedure. Nallathambi put the mixture of carbon black, iron acetate and melamine in a sealed quartz ampule before pyrolysis. However, we heat treated the mixture of carbon black, Fe and nitrogen precursors in an inert flow of nitrogen.

Table 1. Nitrogen atomic percentage of various chemical states

Sample	Total N %	Pyridinic-N	Pyrrolic-N	Quaternary-N
C-N	5.7	62.45	7.53	18.20
Fe-C-N	5.3	54.60	11.43	25.74

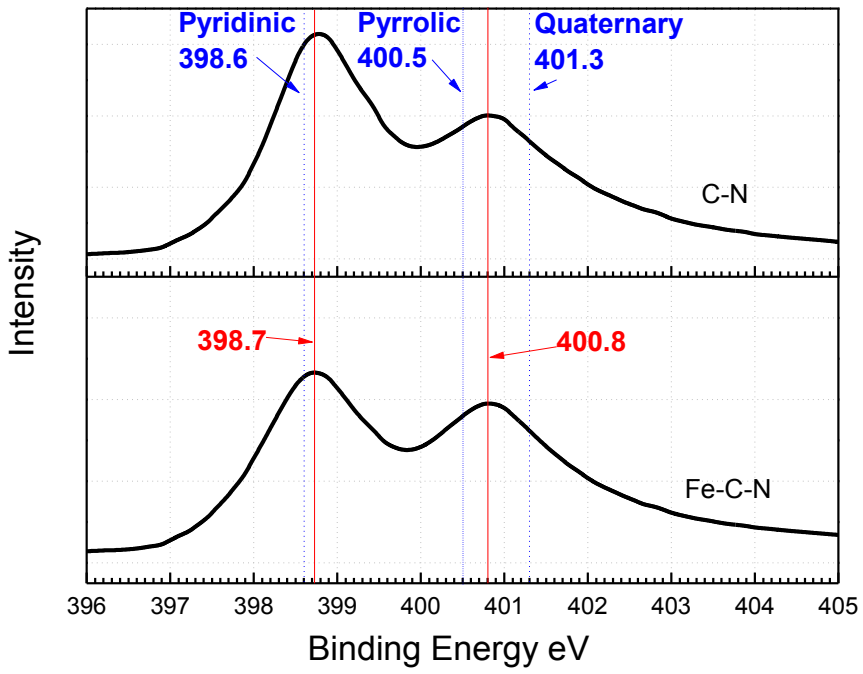

Figure 2. N 1s XPS spectra for Fe-N-C and N-C samples.

3.3 TEM images

The nanostructures of the Fe-C-N catalyst are revealed and displayed in Fig. 3. A high disordered and irregular carbon framework is obtained in our research. It has been reported that the amorphous carbon can be catalytically transformed into graphitic structure at a very low temperature of 600-900℃ by transitional metal [27, 28]. During the pyrolysis, the carbon framework breaks into smaller pieces and surrounds the Fe particles. Fe nanoparticles catalyze the adjacent carbon network into graphitic crystalline. The small broken graphitic sheets will then recombine into some larger fragments. However, due to the presence of Fe particles and the local graphitization, these graphitic sheets are not concentric to each other. Thereby, more disordered graphitic layers with many defects such as dislocations and irregular curvatures will come into being.

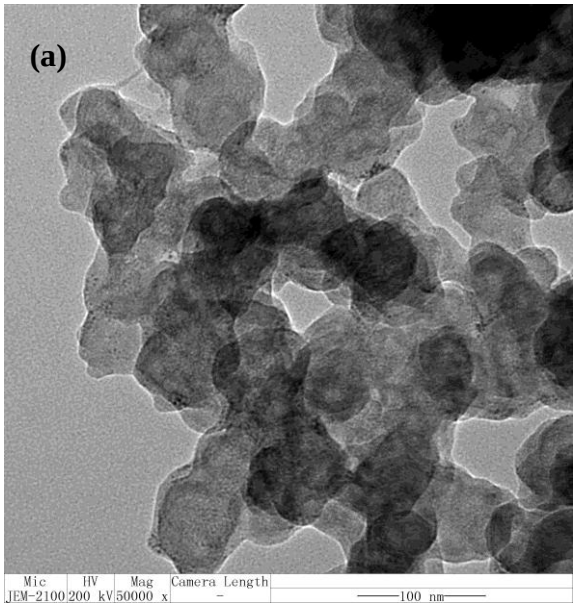

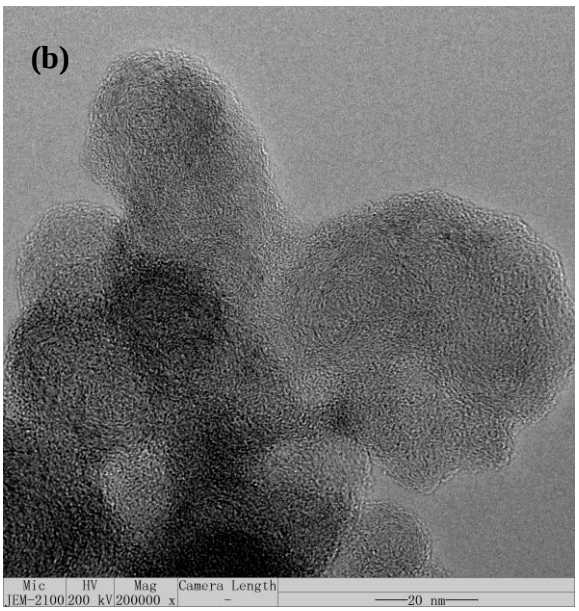

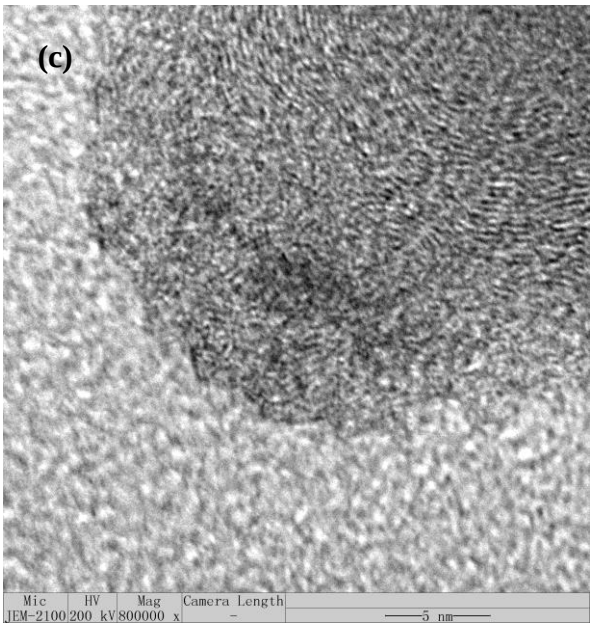

Figure 3. TEM images for Fe-C-N catalyst at various magnifications and areas.

3.4 RDE analysis

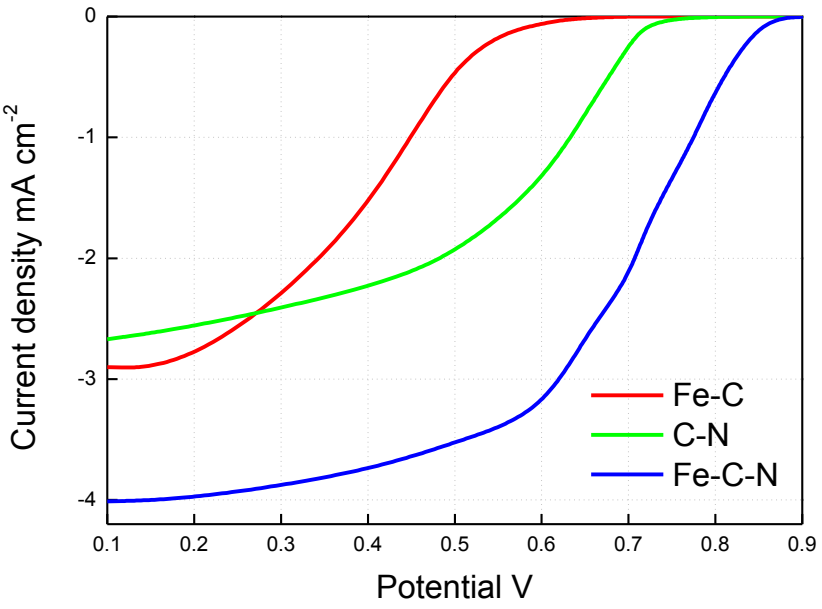

Figure 4. The RDE activity of the catalysts.

The ORR activities for these catalysts are studied using RDE tests and presented in Fig. 4. Heat treatment and doping can improve the ORR activities in varying degrees. The heat treated Fe-C catalyst exhibits some ORR activity evidenced by the onset potential of oxygen reduction at about 0.62 V. However, the substantial improvement is achieved after the incorporation of nitrogen, reflected by an enlarged mass-transport-limited current density at low voltages and a positive shift in the onset ORR potential up to 0.88 V. These enhancements of nitrogen containing catalysts are assumed to be

attributed to the improvement in both intrinsic catalytic activity and the catalytic sites density in the presence of nitrogen components. The Fe-free C-N catalyst also exhibits some ORR activity and the

ORR onset potential is 0.78 V, which is much higher than that of Fe-C catalyst [18, 29-31]. Relative to the metals containing catalysts, the most advantages of metals free C-N catalysts is their high corrosion-resistance and free of metal ions contamination. However, the differences in onset potential show the intrinsic catalytic activity of Fe-C-N catalyst is much higher than that of C-N catalyst. Moreover, the introduction of Fe is likely to catalyze the graphitization during the pyrolysis process and modulate the carbon framework, as addressed in XPS spectra determination. This structural change might produce the farsighted influence on electrolysis.

3.5 Fuel cell tests

Polarization and power density plots for H_2-O_2 fuel cells with the various cathode catalysts are presented in Fig. 5. It can be seen that the fuel cell with C-N catalyst presents a poorer performance at high current density than Fe-C-N catalyst, in good agreement with RDE measurements. The catalyst Fe-C-N exhibits the highest performance and a maximum power density of 418.20 mW cm^{-2} (at 1100 mA cm^{-2}), which is about as much as the performance achieved by Wu [27] and Tang [13].

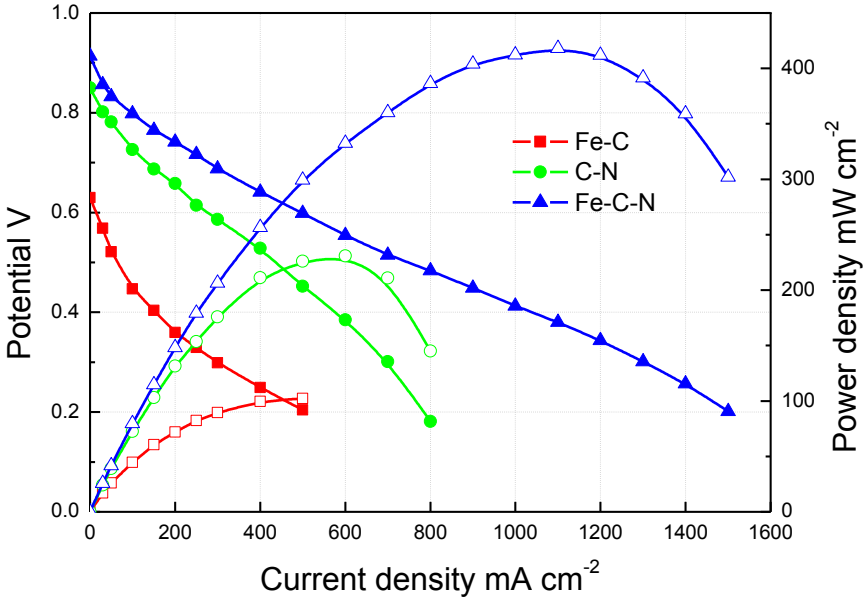

Figure 5. The fuel cell polarization plots of the catalysts.

4. CONCLUSIONS

In summary, we report a Fe based catalyst for ORR synthesized by pyrolyzing carbon supported Fe precursor with melamine at 900 ℃. XRD tests indicate that the carbon framework transforms a better graphitic crystalline structure due to the catalysis of the transition metals. XPS

analysis reveals that the nitrogen atoms are mainly in the form of pyridine-like bonding configuration and facilitate the formation of active catalytic sites. Electrochemical characterizations demonstrate that the Fe-C-N catalyst exhibit excellent electrocatalysis toward ORR. For an actual H_2-O_2 fuel cell system based on this Fe cathode catalyst, the maximum output power density reached 418.20 mW cm^{-2} at 1100 mA cm^{-2}. These results prove that the melamine is a promising nitrogen precursor likely to produce the effective catalyst for oxygen reduction.

ACKNOWLEDGMENT
The authors thank the high school science research project (Grant No: 10KJB480001) of Jiangsu Province, the programs (Grant No: KQ07097) of Huaihai Institute of Technology and the Sci & Tech development project (JSIMR10D05) of Jiangsu-Marine Resources Development Research Institute for financial support of this work.

References

1. M. Winter and R.J. Brodd, *Chem. Rev.*, 104 (2004) 4245.
2. A. Blum, T. Duvdevani, M. Philosoph, N. Rudoy and E..Peled, *J. Power Sources*,117 (2003) 22.
3. Y. Shao, G. Yin, Z..Wang and Y. Gao, *J. Power Sources*, 167 (2007) 235.
4. S.K. Kamarudin, W.R.W. Daud, S.L. Ho and U.A. Hasran, *J. Power Sources*, 163 (2007) 743.
5. J. Zhang, K. Sasaki, E. Sutter and R.R Adzic, *Science*, 315 (2007) 220.
6. V.R. Stamenkovic, B. Fowler, B.S Mun, G. Wang, P.N. Ross, C.A. Lucas and N.M. Markovic, *Science*, 315 (2007) 493.
7. B. Wang, *J. Power Sources*, 152 (2005) 1.
8. L. Zhang, J.J. Zhang, D.P. Wilkinson and H.J. Wang, *J. Power Sources*, 156 (2006) 171.
9. C.W.B. Bezerra, L. Zhang, K. Lee, H. Liu, A.L.B. Marques, E.P. Marques, H.J. Wang and J.J. Zhang, *Electrochim Acta*, 53 (2008) 4937.
10. H.J. Zhang, Q.Z. Jiang, L. Sun, X. Yuan, Z. Shao and Z.F. Ma, *Int. J. Hydrogen Energy*, 35 (2010) 8295.
11. R. Yang, K. Stevens and J.R. Dahn, *J. Electrochem. Soc.* 155 (2008) B79.
12. J. Tian, L. Birry, F. Jaouen and J.P. Dodelet, *Electrochimica. Acta*. 56 (2011) 3276.
13. M. Lei, P.G. Li, L.H. Li and W.H. Tang, *J. Power Sources*, 196 (2011) 3548.
14. K.P. Gong, F. Du, Z.H. Xia, M. Durstock and L.M. Dai, *Science*, 323 (2009) 760.
15. M. Lefèvre, E. Proietti, F. Jaouen and J.P. Dodelet, *Science*, 324 (2009) 71.
16. S. Trasobares, O. Stephan, C. Colliex, W.K. Hsu, H.W. Kroto and D.R.M. Walton, *J. Chem. Phys.*, 116 (2002) 8966.
17. V. Nallathambi, N. Leonard, R. Kothandaraman and S.C. Barton, Electrochemical and Solid-State Letter, 14 (2011) B55.
18. Z.H. Sheng, L. Shao, J.J. Chen, W.J. Bao, F.B. Wang and X.H. Xia, *Acs. Nano*., 5, 4350(2011).
19. G. Wu, L. Li, J.H. Li and B.Q. Xu, *Carbon*, 43 (2005) 2579.
20. Y. Nabae, S. Moriya, K. Matsubayashi, S.M. Lyth, M. Malon and L.B. Wu, *Carbon*, 48 (2010) 2613.
21. G.M. Fuge, C.J. Rennick, S.R.J. Pearce, P.W. May and M.N.R. Ashfold, *Diam Relat Mater*, 12 (2003) 1049.
22. J.W. Jang, C.E. Lee, S.C. Lyu, T.J. Lee and C.J. Lee, *Appl. Phys. Lett*., 84 (2004) 2877.
23. C.P. Ewels and M. Glerup, *J. Nanosci. Nanotechnol*., 5 (2005) 1345.
24. P.H. Matter, L. Zhang and U.S. Ozkan, *J, Catal*., 239 (2006) 83.
25. G. Wu, D.Y. Li, C.S. Dai, D.L Wang and N. Li, *Langmuir*, 24 (2008) 3566.
26. G. Wu, R. Swaidan, D.Y. Li and N. Li, *Electrochim. Acta*., 53 (2008) 7622.

27. G. Wu, M. Nelson, S. Ma, H. Meng, G. Cui and P.K. Shen, *Carbon*, 49 (2011) 3972.
28. O.P. Krivoruchko, N.I. Maksimova, V.I. Zaikovskii and A.N. Salanov, *Carbon*, 38 (2000) 1075.
29. Y. Wang, Y.Y. Shao, D.W. Matson, J.H. Li and Y.H. Lin, *ACS. Nano*., 4 (2010) 1790.
30. Y.Y. Shao, S. Zhang, M.H. Engelhard, G.S Li, G.C. Shao, Y. Wang, J. Liu, I.A. Aksay and Y.H. Lin, *J. Mater. Chem*., 20 (2010) 7491.
31. L.T. Qu, Y. Liu, J.B. Baek and L.M. Dai, *ACS. Nano*., 4 (2010) 1321.